Flip Angle Sensitivity in IR-trueFISP T_1 and T_2 Mapping

R. Newbould[1], R. Bammer[1]

[1]Dept. of Radiology, Stanford University, Stanford, CA, United States

Introduction: An inversion recovery prepared balanced SSFP sequence, known as IR-trueFISP, has recently been proposed as a fast method to quantify T_1, T_2, and spin density (PD) from a single acquisition [1]. Analytical expressions for the signal recovery curve as a function of T_1, T_2, PD, and the flip angle α have been previously determined [1], [2]. In this work, we examine the dependence of the fitted values of T_1, T_2, and PD ($\hat{T}_1$, $\hat{T}_2$, and $\hat{PD}$, respectively) upon the difference between desired flip angle, α, and achieved flip angle $\hat{\alpha}$. The angle achieved is a function of both the excitation slice profile as well as the B_1 field homogeneity. Exact flip angles are difficult to achieve in practice, and often vary over the volume of interest. Furthermore, flat slice profiles require longer excitation pulses, which can lengthen the T_R, enhancing off-resonance effects.

Methods: Bloch equation simulations of the SSFP sequence, using a variety of achieved flip angles versus desired flip angles over a range of T_1 and T_2 values were performed. Analytical expressions were additionally derived from the signal recovery equations for the change in the experimentally determined values.

$$(1)\quad \Delta\hat{PD} = \frac{\sin(\frac{\hat{\alpha}}{2})}{\sin(\frac{\alpha}{2})} \qquad (2)\quad \Delta\hat{T}_1 = \frac{2\cdot\sin(\frac{\hat{\alpha}}{2})\cos(\frac{\alpha}{2})}{\sin(\hat{\alpha})}$$

$$(3)\quad \Delta\hat{T}_2 = \frac{(\sin^2\hat{\alpha})}{\left[\frac{\cos^2(\frac{\hat{\alpha}}{2})}{T_1}+\frac{\sin^2(\frac{\hat{\alpha}}{2})}{T_2}\right]\left[1-\frac{\cos(\frac{\alpha}{2})\sin(\hat{\alpha})}{\sin(\frac{\hat{\alpha}}{2})(\frac{T_1}{T_2}+1-\cos(\hat{\alpha})(\frac{T_1}{T_2}-1))}\right]}$$

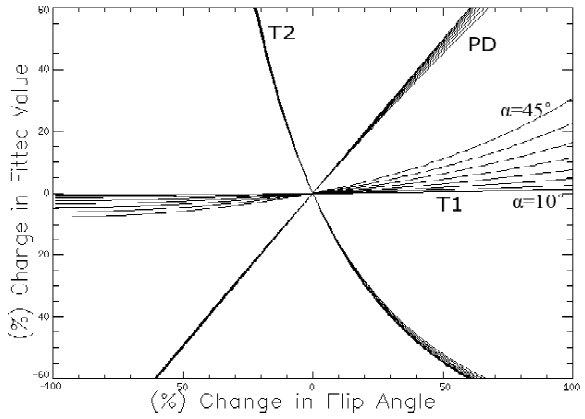

Figure 1. Percent change in fitted value as determined by the Bloch simulations for the three intrinsic parameters as a function of flip angle

An optimized 3-D version of the IR-trueFISP sequence was implemented on a 1.5T GE EXCITE clinical MR scanner using a body coil and a quadrature head coil (GE Medical Systems, Waukesha, WI). Adiabatic non-slice selective inversion and an SSFP preparation period was followed by a train of slab-selective (α=40) profile optimized RF pulses (T_R = 3.84ms, T_E = 1.9ms, FOV=24, matrix=64x64, acq. time=4:03s). Identical coil and phantom setups were also used with a single echo gradient-echo sequence (T_R = 5000ms, T_E = 4.5ms), for the double-angle method [3] to determine the relative flip angle distribution. Here, a single 60° pulse was repeated with a 120° pulse.

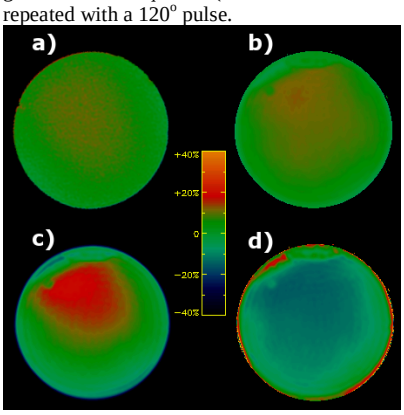

Figure 2. a) Colorized relative flip angle map using quadrature coil from DAM sequence, and IR-trueFISP derived b) T_1 map, c) PD map, and d) T_2 map from an identical setup.

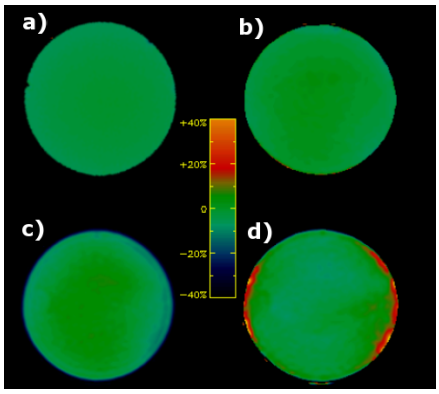

Figure 3. a) Colorized relative flip angle map using body coil from DAM sequence, and IR-trueFISP derived b) T_1 map, c) PD map, and d) T_2 map from an identical setup.

Results: The analytical expressions for the change in the fitted values agree well with the results found via the Bloch simulations. Both the simulations and derived expressions show that the estimated T_2 is extremely sensitive to changes in flip angle. The estimated T_1, however, is relatively insensitive, especially at lower flip angles. An interesting result is that the errors in the T_1 and PD values are not related to the actual T_1 and T_2 values of the medium. Though not readily apparent from the form of (3), the variation in T_2 is sensitive to the T_1/T_2 ratio, though not the absolute values of each.

Parameter fitting was performed on a uniform ball phantom from each IR-SSFP dataset using a nonlinear least squares fitting routine implemented in IDL (Research Systems Inc., Boulder, CO). Additionally, relative flip angle mapping for each was performed using the double angle method (DAM) [3] using the gradient echo data from the same phantom and coil setup. Shown in Figure 2 are the resultant parameter maps from the quadrature head coil, with the relative flip angle map from the DAM on the upper left. A somewhat increased flip angle was noted in an area of the phantom with this setup, which corresponded to increased estimated T_1 and PD values, and markedly decreased estimated T_2 value. Figure 3 contains the results from using the body coil, which is more homogeneous over the same FOV. Improved fits are noted in all parameter maps.

Discussion: The extreme sensitivity of $\hat{T}_2$ to the achieved flip angle can be problematic yet overcome when implementing an IR-trueFISP sequence. While some gain in profile can be attained by using a 3D sequence with optimized slab profile pulses, B_1 sensitivity remains. A smaller coil, such as the transmit/receive quadrature coil tends to have a poor transmit B_1 homogeneity. The use of the body coil for transmit and receive greatly improved the homogeneity, though at the penalty of SNR and possible absolute scaling of the flip angle. The mapping process was noted to be robust to poor SNR. The use of receive-only coils can restore the SNR, though coil coupling / dielectric resonance can be a concern. At higher field strengths, SAR can also become a problem when using the body coil to transmit. From the results of this study, the use of receive-only phased-array coils has been adopted for in-vivo tissue parameter mapping with this sequence. As a secondary note, the dependence of the derived T_1 and PD values solely upon flip angle would in fact give the ability to determine flip angles from the changes in the fits, at least in uniform phantoms. In heterogeneous environments, such as those clinically of interest, the near linear PD variation gives a simple way to map changes in derived PD with changes in flip angle. The achieved flip angle can then be used to fit other parameters, including T_2. The incorporation of a gradient echo readout after the SSFP period for an inherent DAM calculation, or the repetition of the experiment with two flip angles will be explored as a method to additionally map the flip angle, to fully correct the fits.

Acknowledgments: This work was supported in part by the NIH (1R01EB002771), the Center of Advanced MR Technology at Stanford (P41RR09784), the Lucas Foundation, and the Oak Foundation.

References: 1. Schmitt, et. al., MRM(51) 661-667, 2004. 2. K. Scheffler, MRM(49) 781-783, 2003. 3. Stollberger, et. al., MRM(35) 246-251, 1996.